Published in final edited form as:
Circ Res. 2011 March 4; 108(5): 593–606. doi:10.1161/CIRCRESAHA.110.232678.

Molecular imaging of coronary atherosclerosis and myocardial infarction: Considerations for the bench and perspectives for the clinic

Florian Leuschner and **Matthias Nahrendorf**

Abstract

Motivated by the promise to transform preclinical research and clinical care, cardiovascular molecular imaging has made advances towards targeting coronary atherosclerosis and heart failure. We here discuss recent progress in the field, highlight how molecular imaging may facilitate preventive patient care, and review specific challenges associated with coronary and heart failure imaging. Practical considerations stress the potential of fluorescence imaging for basic research and discuss hybrid protocols such as FMT-CT and PET-MRI.

Ground-breaking advances in atherosclerosis and heart failure research have improved our understanding of disease etiology and identified effective therapeutic strategies. Many such discoveries have been translated into the clinical setting and have saved millions of lives. One tangible example is the substantially reduced 30-day mortality of myocardial infarction [1]. Despite this progress; however, today cardiovascular medicine faces greater challenges than ever. Heart failure causes 300,000 deaths per year and has an annual costs of 39 billion US$ [2]. Driven by an obesity epidemic and by improved survival rates of patients with acute MI [3], the number of heart failure patients in the US has risen to a staggering 5.8 million [2].

New approaches that reverse this trend are thus needed to reduce the prevalence of coronary events and improve therapy for patients with coronary heart disease and MI. We increasingly recognize preventive measures as an effective avenue towards this goal. As succinctly put by Dr. Braunwald, "… treating such events is analogous to locking the barn door after the horse has been stolen" [4]. Novel diagnostic solutions that identify individuals at risk could enable early initiation of personalized therapy before irreversible damage occurs. For instance, molecular imaging could identify culprit lesions in the coronary artery tree and initiate treatment to prevent the rupture of the plaque and infarction of the myocardium. Furthermore, imaging has the potential to identify patients with acute MI that are at risk of enhanced remodeling, and to steer yet-to-be-defined therapies that stop this process early before heart failure occurs. Our review focusses on how molecular imaging of the cardiovascular system might contribute to a) preventing myocardial infarction by identifying coronary culprit lesions prior to the ischemic event, and b) preventing remodeling and left ventricular dilation in infarct patients. Ultimately, these advances could strengthen preventive care with the goal of reducing the prevalence of heart failure.

Corresponding author: Matthias Nahrendorf, Center for Systems Biology, 185 Cambridge Street, Boston, MA 02114, Tel: (617) 643-0500, Fax: (617) 643-6133, mnahrendorf@mgh.harvard.edu.

Disclosures
None.

Targets in inflamed coronary plaque

X-ray coronary angiography, which has enabled percutaneous coronary intervention (PCI) in patients with acute myocardial infarction, is an impressive success story. Timely reperfusion therapy results in substantial and sustained survival benefits. That said, the situation is less clear when it comes to PCI that does not target a culprit lesion in acute MI. Several clinical studies failed to show a survival benefit if significant coronary artery stenoses found on X-ray coronary angiography were treated with the aim to restore perfusion deficits [5–7]. Taken together with autopsy results, which suggest that the majority of infarcts are triggered by a culprit lesion of less than 50% lumen loss [8], these studies imply that we possibly treat the "wrong" coronary lesions to prevent ischemic events. Coronary anatomy is an unreliable criterium for identification of atherosclerotic plaque that is at risk of rupture.

Molecular imaging, unlike anatomic imaging, focusses on the immunobiology hidden behind the endothelium and may therefore be able to identify prospective culprit lesions in coronary arteries. Once we can locate an inflamed plaque at risk of rupture, we may be able to use decisive measures, systemically or locally, to prevent myocardial infarction [9]. Imaging biology could also better triage treatment: which lesion should be treated, and which should be left alone? The decision to not implant a stent may avoid unnecessary complications and re-interventions. Thus, there is significant need for next-generation imaging strategies that build on the increased knowledge in vascular biology. Molecular imaging of coronary arteries should be able to assess the regional risk that is specific to a lesion, which can then be used in concert with global risk factors to personalize the therapeutic strategy [10].

The identification of imaging targets has benefited from increased understanding of the inflammatory nature of atherosclerosis. In recent decades inflammation has been shown to have a key role in initiation, maturation and complication of atherosclerotic plaque [11, 12]. In the following, we discuss selected strategies that either show promise for clinical coronary imaging or are well positioned to enhance preclinical drug discovery.

All imaging modalities, including PET, SPECT, MRI, CT, ultrasound and optical imaging, have been used in animal models of atherosclerosis, primarily in apoE$^{-/-}$ and LDLr$^{-/-}$ mice and in hyperlipidemic rabbits. Typically, animals are kept on a high fat diet to accelerate lesion development. The lack of a widely accepted animal model for vulnerable, rupture-prone plaque has been a hurdle[13, 14], but inflammatory lesions, which share important hallmarks with human culprit lesions, serve as reasonable surrogates. Criteria include endothelial denudation, high macrophage content, presence of foam cells, a thin fibrous cap, and a lipid or necrotic core, among others [15] (Figure 1). Since rodents' coronary artery tree is extremely small, the aorta has been used as an alternate vascular target region to model coronary imaging in humans. In mice, the aorta's diameter is about 1 mm, which is comparable to small coronaries in humans. For serial imaging studies, it is important to locate the target region previously imaged. Anatomic landmarks, such as the aortic root, can serve as guides. In apoE$^{-/-}$ and LDLr$^{-/-}$ mice the aortic root is particularly suitable because it features high plaque loads and is distant from the liver and the kidneys, organs that excrete imaging agents and therefore often have high background signal.

Atherosclerotic plaque begins with recruitment of circulating leukocytes, predominantly monocytes, to the vessel wall. The recruitment process is driven by chemokines such as MCP-1 and fractalkine, and by adhesion molecules that are expressed by endothelial cells [12]. Adhesion molecules on endothelial cells bind ligands on the surface of rolling leukocytes. Adhesion molecule expression is limited to activated endothelium that either lines an inflamed plaque, or is located at a site of lesion initiation. Understanding of the

leukocyte recruitment mechanism has resulted in particular interest in imaging selectins, integrins, and Vascular Cell Adhesion Molecule-1 (VCAM-1), all of which are in direct contact with the imaging agent circulating in the blood pool. Antibodies and peptides have served as affinity ligands [10, 16], and nuclear (Figure 1) [17], ultrasound [18] and MR imaging [19] detected the respective reporter moieties.

Inflammatory cells residing in the plaque, in particular monocytes, macrophages, and foam cells, are excellent imaging targets because they play an important role in the evolution and complication of atherosclerosis [12]. After recruitment, these cells scavenge lipids, secrete cytokines that further amplify inflammation, and produce proteases such as metalloproteinases and cathepsins. In concert with the inflammatory cells' phagocytic function, proteases destabilize the plaque by damaging the extracellular matrix and thinning of the fibrous cap [12]. Targeted imaging of macrophages is based on their phagocytic function. Differently sized and composed nanoparticles are readily taken up by monocytes and macrophages [16, 20]. This mechanism has been exploited using a variety of nanomaterials. Typical labels for MRI detection of these nanoparticles include liposome-encapsulated Gd-DTPA that increases T1 contrast -- bright signal [21] -- and ultra small superparamagnetic iron oxide (USPIO) nanoparticles that enhance T2* contrast -- dark signal [22–24]. Nanoparticles have also been labeled with isotope reporters, including Fluorine-18 [25] and Copper-64 (Figure 1) [26].

Proteases are attractive imaging biomarkers due to their role in plaque destabilization [12]. They have been targeted with two major strategies. Nuclear imaging probes, which could be used in non-invasive coronary imaging in patients, are based on small-molecule protease inhibitors [27, 28]. These bind to the active site of the enzyme and enrich in tissue that has a high protease content. An alternative approach uses an optical pro-drug that is activated when it comes into contact with proteases [29, 30]. The enzymes cleave defined peptide sequences, liberate the attached fluorochromes and thereby render them fluorescent. Only these liberated fluorochromes can be excited with a laser, and the resulting emission is recorded as a measure of enzyme activity [31]. The ability of one enzyme to activate several reporter moieties acts as an efficient amplification mechanism. Fluorescence molecular tomography (FMT) has resolved this process non-invasively in mice (Figure 1) [30]. Physical hurdles likely preclude using FMT to assess coronary arteries in patients. Instead, clinical fluorescence imaging may be pursued with intravascular catheters, which are inserted into the vascular lumen and sense protease activity in the adjacent vessel wall [32]. Current catheter prototypes are small enough to be used in coronaries and combine white light angioscopy with two-dimensional fluorescence imaging in the near infrared [33]. While invasive, this approach may be useful to supplement the anatomic information obtained by X-ray coronary angiography with a biological read-out.

Additional molecular targets with promise for imaging atherosclerotic plaques in the coronary artery tree are integrins upregulated in angioneogenesis [34–36], myeloperoxidase [37], clotting-related biomarkers such as fibrin [38] and platelets [39, 40], and lipid components of the plaque [41].

While the technologies discussed above are currently negotiating the discovery pipeline, ^{18}F-Fluorodeoxyglucose (^{18}F-FDG) has been used to image coronary arteries in patients with PET-CT (Figure 1) [42–44. ^{18}F-FDG is a glucose analog in which an oxygen atom is replaced with Fluorine-18, a PET isotope with a half life of 110 minutes. Due to its uptake in analogy to glucose, ^{18}F-FDG enriches in cells with high metabolic rates. Once inside the cell, ^{18}F-FDG is phosphorylated and becomes trapped [45]. Originally, this imaging technique has been designed to follow metabolically active tumor cells. While it has been very successful, an emerging limitation for oncologic imaging is that ^{18}F-FDG is not

specific to cancer cells. Recruitment of inflammatory host cells to the site of primary and metastatic cancer may also increase ^{18}F-FDG signal [45]. Likewise, inflammatory atherosclerotic plaques are metabolically active tissue, and therefore show high signal on PET images. Several studies have correlated the ^{18}F-FDG signal to the number of macrophages in a lesion [46, 47]; however, ^{18}F-FDG is not specific to these cells either. The clinical availability of ^{18}F-FDG PET creates an opportunity to overcome the considerable technical difficulties of imaging a small, fast moving target in coronary arteries with this modality.

Noninvasive coronary molecular imaging: What modality, when and for whom?

There are specific hurdles associated with each modality for imaging atherosclerosis in coronary arteries (Table 1). The plaques in these vessels are small, move rapidly with the heart and respiration, and are close to tissue interfaces with lung, blood and myocardium, all of which can lead to artifacts or background signal. In addition to its high spatial and temporal resolution for anatomic imaging, MRI shows promise for molecular imaging in the coronary arteries, despite its somewhat lower sensitivity in comparison to PET. High sensitivity translates into low agent doses, which in turn reduces toxicity concerns. While PET is the most sensitive and quantitative modality, it has a limited spatial resolution (~4 mm clinically, ~1 mm in small animal imaging). Unfortunately, physical constraints make it unlikely that PET's spatial resolution will improve further. A positron travels a considerable distance from emission by the isotope -- the location of the probe -- until annihilation during collision with an electron creates the gamma ray detected by the PET ring -- the location of imaging signal. Partial compensation for limited spatial information can be achieved through combination with an anatomic modality. There have also been reports of CT agents that target vascular inflammation [48]. The excellent spatial resolution and the recently discussed potential of multispectral CT imaging [49] make this modality attractive, even though it is less sensitive to molecular markers than PET or MRI. It should be noted that coronary CT can cause considerable exposure to radiation (3–16 mSv) [50]. Newer devices can reduce the overall exposure from PET-CT to < 10 mSv [51]; however, this is still considerable exposure that precludes uncritical use for screening in lower-risk individuals. For comparison, the exposure caused by a chest x-ray is 0.1 mSv, a sestamibi stress test is 9 mSv, and a coronary catheterization is 7 mSv [50].

Once molecular imaging tools that assess coronary atherosclerosis become available for use in patients, we will need to analyze their clinical value, including considerations on radiation exposure mentioned above. Clinical trials will investigate how a specific imaging tool improves decision making and outcome, and assess cost-benefit ratios. Routine imaging should only be adopted after these data have been collected and appropriate patient selection procedure has been determined. A recent editorial proposes a possible scenario for integrating coronary imaging into clinical care to improve risk assessment and guide therapy [4]. Global risk assessment using tools such as the Framingham risk score should precede imaging, resulting in low, intermediate and high risk cohorts. The latter comprises one-sixth of the adult population, who have a >2% chance of an event within the next year. Within this population, it could be beneficial to identify individuals at very high risk and regionalize risk by identifying specific vulnerable coronary plaques. These patients may then benefit from intense global risk factor reduction, medical therapy aiming at cooling down of inflamed coronary lesions [15], and local therapy such as implantation of drug eluting stents [52] or preventive coronary bypass surgery [4]. Because imaging technology targeting vulnerable plaque is a fairly recent development, our knowledge on the fate of vulnerable plaques is still limited. This renders considerations on therapy, while very important, also extremely speculative. For instance, there is a paucity of prospective clinical studies that

investigate the fate of individual vulnerable plaques over time. An important aspect is the number of vulnerable plaques in an individual patient. If vulnerable plaques were predominantly short lived, would frequently resolve spontaneously, if there were too many such lesions in one patient, and if only a subset resulted in infarcts, local therapy may not be reasonable. Autopsy [53] and intravascular ultrasound studies [54] suggest occurrence of more than one and up to 5 vulnerable lesions at a given time.

Imaging targets in heart failure

Even when above considerations may have turned into clinical reality, it is unlikely that they achieve complete prevention of myocardial infarction. Thus, for patients with acute MI, we need additional tools to identify individuals that will undergo accelerated remodeling and have a high risk of developing heart failure. Anatomic imaging is already an integral element of the care provided after MI [55]. Patients undergo serial echocardiography, and MR and nuclear imaging are used to measure function, perfusion and infarct size. The prognostic value of infarct size is widely recognized. While mortality has been the corner stone of drug efficacy trials, imaging is increasingly used to follow surrogate endpoints related to left ventricular volumes and function. However, many of these parameters change late in the course of disease. When a patient's EF has declined to 20%, there is little we can do to return it to normal, with the exception of heart transplantation. To enable preventive measures we will need upstream biomarkers that allow us to intervene before disease has progressed beyond the point of no return. In the following, we will discuss selected molecular imaging techniques in the sequence of disease progression, starting with the initial injury.

Within hours of ischemia onset, myocytes begin to die from necrosis and apoptosis (Figure 2). While delayed enhancement MRI after injection of Gd-DTPA yields an excellent high-resolution image of myocyte loss and infarct size, it cannot differentiate between necrosis and apoptosis. Apoptosis is a reversible process, and thus a therapeutic target, whereas necrosis is not. A number of apoptosis imaging approaches have been proposed, most of which involve the use of annexin-V as an affinity ligand [56–59]. Annexin-V binds to phophatidylserine (PS), a molecule that flips to the outside of the cell membrane. An elegant approach proposed by Sosnovik combined MR imaging of apoptosis with an annexin-V decorated nanoparticle and delayed enhancement MRI in a mouse model of cardiac ischemia (Figure 3) [60]. Here, identifying necrotic versus apoptotic myocardium was possible because T1-weighted delayed enhancement after injection of Gd-DTPA enhanced the entire infarct, whereas T2* signal changes due to nanoparticle binding reported on apoptotic myocardium only. MR agents that bind to exposed DNA are also being developed [61]. Apoptotic myocytes have been imaged in patients with chronic heart failure by SPECT after injection of Technetium-99m-labeled annexin-V [62].

Injury to the myocardium triggers an inflammatory response which initiates the wound healing process [63]. An initial neutrophil surge is followed by monocytes, which are recruited in large numbers from their splenic reservoir [64] and the bone marrow. These cells are essential for proper repair (Figure 2), and their either insufficient or excessive presence in the infarct may impair wound healing, increase infarct expansion, and consequently enhance LV dilation [65]. Two monocyte subsets are recruited to the heart sequentially [66]. In the mouse, inflammatory Ly6-C^{high} monocytes dominate on days 1–3 and promote removal of debris. Thereafter, Ly6-C^{low} monocytes promote tissue repair and resolution of inflammation [66]. A similar biphasic pattern, with an initial peak of inflammatory $CD16^{-}$ monocytes, was also reported for blood monocyte levels in patients with acute MI [67]. Monocytes' central role in infarct healing [65] make these cells interesting imaging targets. Imaging may detect excessive or prolonged inflammation after MI, and so identify

individuals at risk for progressive remodeling. This hypothesis has been tested in preclinical studies, in which monocyte/macrophage imaging was combined with serial MR volumetry [68]. Mice with increased monocyte/macrophage signal on day 5 after coronary ligation had worse ejection fraction on day 21, despite similar initial infarct size. In patients, monocyte/macrophage content in infarcts has not yet been directly imaged, however, blood levels of the inflammatory $CD14^{+}CD16^{-}$ subset were inversely correlated with MRI-derived ejection fraction 6 months after MI [67]. Imaging tools that non-invasively report on these cells' presence could serially follow the myeloid cell flux from the bone marrow and spleen [64] towards the injured heart and thus enhance understanding of system kinetics [65]. This, in turn, will help to identify how monocyte/macrophage responses can be modulated therapeutically.

T2*-weighted MRI can follow uptake of iron oxide nanoparticles by macrophages [69], an attractive approach because MRI also reports on wall motion and global heart function (Figure 2 and 4). Fluorescent labeling of nanoparticles has precisely determined nanoparticles' cellular uptake profile by microscopy and FACS. After digestion of infarct tissue, the cell suspension retrieved from infarcts was stained with a cocktail of fluorescently labeled antibodies in order to identify cells of interest by their specific surface marker expression [66]. In a separate channel of the flow cytometer, the fluorescence intensity of the nanoparticular fluorochrome label in each cell type -- i.e. the cellular uptake of the probe -- was then quantified. With certain nanoparticle preparations, over 80% of the signal is derived from monocytes/macrophages. Timing of the imaging (i.e. day after coronary ligation, injection-imaging sequence) may influence the uptake profile [70].

Macrophage presence in the infarct has also been imaged by MRI after injection of ^{19}Fluorine-labeled liposomes (Figure 4) [71. ^{19}F MRI does not rely on protons, which are abundant in the body as part of water, as a signal source. Unlike Gd- or iron oxide-based MR agents, which indirectly modify signal by accelerating proton relaxation, ^{19}Fluorine is imaged directly. Because it does not naturally occur in the body, the background signal in this imaging technique is very low, as only ^{19}F incorporated in the imaging agent is detected. Typically, ^{19}F is combined with ^{1}H MRI for anatomical co-registration (Figure 4). On the downside, ^{19}F MRI lacks the typical amplification mechanism of Gd or iron oxide, in which one moiety of agent interacts with many surrounding protons. Thus, the sensitivity of ^{19}F MRI could be lower than that of ^{1}H MRI.

Comparable to the strategy of ^{18}F-FDG PET imaging of inflammatory atherosclerosis, French et al. have followed inflammation in a mouse after myocardial ischemia with ^{18}F-FDG (Figure 4) [72]. The high background uptake of the myocardium is a hindrance in cases where the ischemic area is not well defined, especially since ischemia shifts myocardial metabolism towards increased glucose utilization [73]. Nanoparticles labeled with PET isotopes such as ^{64}Cu are not taken up by myocytes and may thus be a suitable tool to quantify post-MI inflammation [26]. Current efforts aim at developing clinically viable nanoparticle PET reporters [25, 74].

Ultrasound imaging is a less quantitative but very cost-efficient modality and has been employed for macrophage imaging with lipid microbubbles (Figure 4). These microbubbles are retained in phagocytes in the myocardium [75] and may thus facilitate bedside estimation of inflammatory macrophage content in a patient's infarct.

Monocytes/macrophages synthesize and secrete a wealth of cytokines and enzymes, including proteases. In acute MI, matrix metalloproteinases and cathepsins participate actively in the wound healing process [76]. They digest the preexisting extracellular matrix and so enable the generation of granulation tissue and formation of a stable scar. Their

function is delicately regulated between protease generation, activation and inhibition by TIMPs (Tissue Inhibitor of Metalloproteinases) [77]. If the balance of matrix degradation and synthesis is disturbed, infarct healing is impaired, and this may result in ventricular rupture or infarct expansion. In later stages of left ventricular remodeling, these enzymes also attack the extracellular matrix in the remote, non-infarcted myocardium and promote ventricular dilation [78]. The same molecular agents used for imaging in inflamed atherosclerotic lesions, as described above, have also been used to characterize proteases in myocardial infarction by SPECT [79] and fluorescence imaging (Figure 2) [68, 70, 80]. These studies reported increased activity after MI, which, if too high, may counteract matrix generation, favor infarct expansion and thus contribute to ventricular dilation. A typical example of how increased protease activity worsens outcome can be seen in a study that investigated infarct healing in apoE$^{-/-}$ mice [68]. Due to their atherosclerotic "comorbidity", which implies higher monocyte blood levels, apoE$^{-/-}$ mice show increased and prolonged monocyte recruitment to the heart, increased protease activity, prolonged infarct inflammation, and accelerated LV dilation. Myeloperoxidase (MPO), which also serves as a biomarker for inflammatory monocytes and neutrophils in ex vivo clinical pathology, is an inflammatory enzyme that has been imaged after MI with the activatable T1-targeted MRI agent MPO-Gd (Figure 2) [81]. In addition, MPO-Gd enhances rejecting heart transplants [82]. The probe is based on a Gd-encaging chelator derivatized with serotonin moieties. If in contact with the target enzyme, the serotonin residues are radicalized and react with each other and the surrounding matrix, which leads to delayed wash out kinetics and higher signal intensity on T1-weighted MRI [83]. While MPO content is even higher in neutrophils [82], this approach can, with the right timing, be used to follow inflammatory monocyte levels in the infarct. A fluorescent nanoparticle-based sensor for peroxynitrite ($ONOO^-$) and myeloperoxidase mediated hypochlorous acid ($HOCl/OCl^-$) production has been used to sense inflammation in infarct tissue [84], however this approach has not yet been evaluated for in vivo imaging.

The extracellular matrix is a tissue component that preserves the structure of the heart. A delicate network of collagen fibers, linked to each other and to cells via integrins, supports the left ventricular geometry. Because it weakens this network, increased protease activity favors ventricular dilation [78]. On the other hand, over-abundant collagen is also harmful because it hinders diastolic function. In addition, the extracellular matrix lends stability to the infarct scar, which prevents rupture and/or infarct expansion. Several imaging approaches directly target components of the extracellular matrix (Figure 2). A technetium-99m-labeled RGD peptide was used to image $\alpha_v\beta_3$ integrin expression in mice after myocardial infarction [85]. The highest uptake was observed 2 weeks after coronary ligation in the infarct, whereas the signal was higher in the remote myocardium at 12 weeks. The signal was colocalized with myofibroblasts, which are important producers of collagen. This study detected the effects of pharmacological inhibition of angiotensin-2, a peptide with known pro-fibrotic activity. These data suggest that it is possible to image active construction of the extracellular matrix, as integrin expression declines in a mature scar. The same agent was then used in 10 patients with myocardial infarction in conjunction with delayed enhancement MRI [86]. In this first-in-human study, integrin SPECT signal at 3 and 8 weeks colocalized with the infarct scar on follow-up MRI 1 year after the ischemic event. The findings on SPECT-positive area as well as signal intensity were heterogeneous. Future clinical studies will explore the predictive value of these data. A similar peptide, labeled with the PET isotope Fluorine-18 (^{18}F-Galakto-RGD), has been used in a patient 2 weeks after MI [87]. The authors describe that the likely target is integrin expression due to angiogenesis in the healing infarct, based on a study in rats after coronary ligation [88]. A wealth of publications describe the use of the RGD peptide to target angiogenesis in the setting of atherosclerosis [89] and cancer [90]. In addition, integrins are also expressed by leukocytes, which are abundant in the wound shortly after MI. Thus, while RGD-based

probes have high affinity to integrin, imaging timing is essential because the manifold cellular source of integrin expression varies while disease progresses.

Once collagen fibers are synthesized, they are crosslinked into an interconnected matrix. Tissue and plasma transglutaminases (FXIII) are involved in this process. FXIII$^{-/-}$ mice showed an increased ventricular rupture rate after coronary ligation [91]. FXIII's role in infarct healing was also suggested by two clinical observations: patients that died due to infarct rupture had lower FXIII protein content in the infarct when compared to a control cohort [92]. Furthermore, a study that analyzed the FXIII genotype and followed acute MI patients over time suggested a protective effect of a FXIIIA-V34L mutation associated with increased FXIII activity [93]. A FXIII targeted imaging probe, which is based on a transglutaminase substrate peptide labeled with Indium-111, was used to study infarct healing in mice after myocardial infarction (Figure 2). Decreased FXIII SPECT signal in the infarct associated with accelerated left ventricular dilation, suggesting that this probe could be used to predict prognosis [92]. Collagen was also imaged directly in rats 6 weeks after coronary ligation [94]. A Gd-based T1 shortening probe that relies on a cyclic peptide as an affinity ligand to collagen [95] caused strong enhancement and delayed wash out of the agent from the infarct scar (Figure 2). Other imaging strategies used to investigate heart failure include imaging of therapeutic targets (angiotensin-2 receptors [96], beta-receptors [97]), sympathetic innervation [97, 98] and imbalances in myocardial metabolism (we refer to a recent comprehensive review by Peterson and Gropler) [73].

"How-to" considerations for bench research

Anatomic and molecular imaging are attractive research tools because their non-invasive character enables serial studies. In the lab, a molecular imaging biomarker often represents a molecule or cell that is central to system regulation and is thus a possible therapeutic target. A noninvasive tool that can quantitate a regulatory molecule or cell would allow its serial investigation, for instance before and after a therapeutic intervention. Imaging may quantify such a target, and because the animal survives, one can later obtain ejection fraction in the same individual to study impact on outcome and prognostic value [68, 92, 99].

The investigation of biology in the undisturbed in vivo environment prevents many artifacts introduced by in vitro techniques. Some dynamic phenomena, such as cell-to-cell interactions, are only accessible via in vivo imaging; cell-to-cell interactions, to continue with the specific example, require in vivo microscopy. The advantages of in vivo methodologies have resulted in an increased interest in imaging to supplement invasive and ex vivo techniques in basic science.

Some imaging techniques, such as echocardiography in mice [100], have already been embraced by a large research community. The example of echocardiography shows what is required to broadly disseminate imaging: the tool must be straight-forward, capable of high throughput, and cost effective. Unfortunately, more technology-intensive modalities like MRI and PET do not meet these criteria. These scanners are expensive to purchase, and their operation and maintenance requires expertise and sustained financial commitment. The higher costs of equipment and required on-site expertise will likely limit widespread installation of these devices. One possible solution is the creation of centralized facilities that make their services available to outside collaborators. Supported by specific grant mechanisms from the National Cancer Institute, this strategy has been successfully implemented for cancer imaging. Dedicated cardiovascular imaging centers would likely advance the use of molecular imaging tools in basic cardiovascular research, share the financial burden, and make these technologies more accessible to the community.

Wider dissemination of a modality beyond imaging centers requires “push button” ease of use, limited costs, and seamless integration with traditional lab techniques. Optical imaging has matured to fulfill these requirements [101] and is therefore attractive for scientists without extensive expertise in imaging. In comparison to other modalities, optical imaging equipment is less expensive to buy and to maintain, as it does not require radiation permits, shielding, and cryogen fills. Optical imaging agents are harmless and non-toxic, do not decay and can be stored on the shelf. As shown in Figure 5, optical imaging is highly versatile and spans applications with high spatial resolution, such as intravital microscopy, to applications with high sensitivity capable of non-invasively probing molecular targets, as with bioluminescence and FMT.

A decisive advantage of fluorescence imaging is its capacity to integrate well with traditional lab techniques. For instance, microscopy and FACS can measure fluorescent molecular agents following in vivo imaging (Figure 5). The multichannel capabilities of optical imaging, which are already widely exploited in multicolor flow cytometry or immunofluorescence histology, are increasingly used in vivo to interrogate several targets simultaneously. This allows investigators to pursue systems approaches not limited to a single biomarker. Examples for multichannel imaging are shown for intravital microscopy and FMT (Figure 5).

Role of multimodal imaging: preclinical

Imaging modalities are complementary. Nuclear imaging has a limited spatial resolution, CT has low sensitivity to molecular targets, MRI is often semiquantitative, and optical imaging can not penetrate more than ~5–8 cm of tissue [89]. Combining modalities can compensate for some of these limitations while building on their respective strengths (Table 1). This is particularly important in the heart, a challenging imaging target with fast moving, small structures. A modality with high resolution and good soft-tissue contrast can provide anatomical structures while a second, more sensitive modality may sample molecular information.

An example how advantages can be gained from fusing modalities is the combination of X-ray CT with Fluorescence Molecular Tomography [30, 68, 74, 99]. Like PET imaging, FMT is quantitative and sensitive [74] but provides limited anatomical information. Stand-alone FMT imaging is sufficient in large targets such as subcutaneously implanted tumors. Vascular and myocardial FMT, however, benefit from adding a modality that provides precise anatomic information. Two strategies have been proposed. An integrated FMT-CT device that combines laser, CCD cameras and X-ray source on one gantry [102] facilitates the use of CT priors for improved image reconstruction of FMT data sets [103]. An alternative approach uses separate devices. Here, the animal is transferred from the FMT imager to the CT or MRI scanner and image fusion is based on fiducials incorporated in an imaging cassette holding the anesthetized mouse. The advantage of the second approach lies in its versatility. It allows integration of any modality (FMT with PET, CT, MRI, or multiple combinations). Spectrally-resolved FMT provides several channels for simultaneous quantification of molecular markers. In the commercially available system the excitation/emission wavelengths are 635/655 nm, 680/700 nm, 750/780 nm, and 785/815 nm. Theoretically, PET and MRI could be added to yield a total of 6 channels. The most complex study to date combined 3 FMT channels with PET and CT and indicates that hybrid imaging of multiple targets is feasible [74]. For instance, an infarct imaging study could use both the commercially available FMT system and probes, to quantify myocyte apoptosis, monocyte/macrophage numbers, protease activity, and integrin expression, and MRI, to measure collagen content [94], in one single study. These parameters could then be followed over time, and correlated to LV function and infarct size. Such a multimodal protocol would provide

insight into the generation of heart failure on a systems level by following a network of inter-dependent biomarkers. The use of quantum dots as fluorescence reporters may add even more channels, because these materials' emission profiles are narrow [104]. Another interesting development is the quantitation of near infrared reporter proteins by FMT [105], which could be used to investigate gene expression or stem cell survival in the cardiovascular system in concert with the biomarkers noted above.

Role of multimodal imaging: clinical

Multimodal scanners combine two or more modalities and fuse the resulting images, as, for instance, in PET/CT imaging of coronary atherosclerotic plaque (Figure 6a). Here, the limited spatial information derived from PET is overcome by the addition of anatomic CT, which helps to localize PET signal (but does not necessarily improve PET's spatial resolution or solve the issue of partial volume effects). While the integration of PET with MRI is particularly promising for imaging the heart, the engineering challenges are higher than in PET/CT due to the required non-magnetic MRI environment. Experimental systems that feature a PET ring inside the magnet allow simultaneous acquisition in both modalities [106, 107]. This integration represents a break-through for functional brain imaging, in which simultaneous MRI and PET (e.g. fMRI for blood oxygenation in combination with disease-targeted PET probes) can provide novel insight. Unlike in multimodal functional brain imaging, the time component may be less important in cardiovascular imaging. Here, MRI and PET could be done consecutively as in PET/CT, somewhat lowering the technological hurdles because the PET ring would not have to reside inside the magnet. There are a number of arguments for the particular synergy of cardiovascular PET/MRI. First, using MRI instead of CT reduces radiation exposure, which is of paramount importance for the preventive approaches discussed in this review. Second, cardiovascular MRI is highly versatile and very powerful. It can identify precise anatomical structures and physiological parameters -- including coronary anatomy, cardiac volumes, regional wall motion, global heart function, infarct size, perfusion, and myocardial strain [108–110] -- with excellent temporal resolution. A possible clinical scenario for coronary PET/MRI is the detection of plaque inflammation by PET (with ^{18}F-FDG now, and in the near future with agents such as ^{18}F-RGD[111], the VCAM-1 targeted probe ^{18}F-4V[17] or macrophage targeted nanomaterials[26]). The molecular information can then be fused with MR coronary angiography, which reports the degree of stenosis and composition of the plaque [112]. In addition, MRI can quantify downstream physiological effects such as perfusion (using first pass or spin labeling techniques) and wall motion (using cine or phase contrast), and identify an infarct scar (using delayed enhancement) [108, 109]. Similar scenarios can be envisioned for patients after MI: coronary status, infarct size and LV function are determined by MRI [108, 109], and a wound healing biomarker that predicts remodeling is tracked by PET. Figure 6b shows an example of multimodal imaging in heart failure. Wound healing was imaged with an integrin-targeting nuclear tracer, while anatomy was followed by MRI. This study [86] did not combine both modalities in one session, but nevertheless illustrates the clinical potential of multimodal imaging.

Clinical promise

The need for spatially resolved, patient-individualized risk assessment is driving the molecular imaging field towards clinical translation. The near future will likely see several molecular agents entering the clinical phase of development. The track record of nuclear tracers that are in clinical use, many of them in cancer imaging, positions PET as a modality that, in conjunction with CT and MRI, will assess inflamed coronary plaque and molecular events in remodeling and heart failure. A number of nuclear imaging agents have already been used in patients with heart disease, including agents targeting integrin expression [87, 96],

apoptosis [62], and metabolic activity (^{18}F-FDG) [42–44]. The promise of nuclear imaging lies in its high sensitivity and the design aspects of PET tracers. These often consist of a peptide and an isotope, whereas MR agents are more complex due to the need for signal amplification. However, the appeal of imaging techniques that do not cause radiation exposure and feature good spatial resolution favors MR, ultrasound and optical imaging. Cardiovascular MRI [110], in particular, is undergoing rapid technical advances that will increase acquisition speed, signal to noise ratio and sensitivity [113].

Will we be able to afford clinical molecular imaging? The increasing number of imaging procedures contribute to exploding costs in health care. Nevertheless, integrating molecular imaging into clinical decision-making with the goal of disease prevention should be cost effective. A procedure detecting a vulnerable plaque could result in intervention that prevents deleterious -- and costly -- events. Care for a patient with acute MI or heart failure includes admission to the hospital, coronary catheterization, possibly an implantable defibrillator and perhaps even heart transplantation, all of which outweigh the cost of imaging by several orders of magnitude.

Conclusion

Motivated by the potential to transform preclinical research and clinical care, cardiovascular molecular imaging has made advances towards targeting coronary atherosclerosis and heart failure. Technology-driven proof of principle studies are abundant, have reached key technology milestones (Figure 7), and illustrate the promise of molecular imaging. In the next decade, our rapidly growing knowledge in cardiovascular biology promises identification of advanced targets, which will likely represent central check-points of pathophysiological systems (Figure 7).

Basic research is increasingly integrating imaging data, while optical techniques hold particular promise for dissemination into non-imaging laboratories. The synergy created by multimodal imaging, in particular PET/MRI, will unite molecular and physiologic information. ^{18}F-FDG PET/CT is a clinically available tool currently being explored for coronary imaging. Imaging will become an integral part of clinical trials, in which imaging biomarkers may serve as surrogate endpoints. However, formidable hurdles to clinical translation still exist. To overcome these, the cardiovascular community can learn from the cancer field, which is quickly adopting imaging for both bench work and clinical translation. Dedicated grants have funded large imaging centers that combine expertise across medical physics, cancer biology, and probe chemistry. Basic scientists without extensive imaging expertise profit from this infrastructure, using high-end imaging tools on a collaborative base. Similar efforts in cardiovascular science could replicate this success.

Acknowledgments

We gratefully acknowledge Drs. Juhani Knuuti, John Chen and Claudio Vinegoni for providing previously unpublished image material. We acknowledge Drs. Filip K. Swirski, Mikael J. Pittet, David E. Sosnovik and Ralph Weissleder for fruitful discussions.

Funding Sources

This work was funded in part by NIH grants R01HL095629, R01HL096576, R01EB006432, HHSN268201000044C, American Heart Association SDG0835623D, and the Deutsche Herzstiftung e. V.

Non-standard Abbreviations and Acronyms

CCD	charge coupled device

CT	X-ray computed tomography
Gd	Gadolinium
FACS	Fluorescence Activated Cell Sorting
FDG	Fluorodeoxyglucose
FMT-CT	Fluorescence Molecular Tomography in conjunction with X-ray Computed Tomography
FXIII	Factor XIII (plasma transglutaminase)
IVM	Intravital Microscopy
MPO	myeloperoxidase
MRI	Magnetic Resonance Imaging
Mφ	Macrophage
PCI	Percutaneous Coronary Intervention
PET	Positron Emission Tomography
PS	Phosphatidylserine
SPECT	Single Photon Emission Computed Tomography
Sv	Sievert

References

1. Krumholz HM, Wang Y, Chen J, Drye EE, Spertus JA, Ross JS, Curtis JP, Nallamothu BK, Lichtman JH, Havranek EP, Masoudi FA, Radford MJ, Han LF, Rapp MT, Straube BM, Normand SL. Reduction in acute myocardial infarction mortality in the United States: risk-standardized mortality rates from 1995–2006. JAMA. 2009; 302:767–773. [PubMed: 19690309]
2. Lloyd-Jones D, Adams RJ, Brown TM, Carnethon M, Dai S, De Simone G, Ferguson TB, Ford E, Furie K, Gillespie C, Go A, Greenlund K, Haase N, Hailpern S, Ho PM, Howard V, Kissela B, Kittner S, Lackland D, Lisabeth L, Marelli A, McDermott MM, Meigs J, Mozaffarian D, Mussolino M, Nichol G, Roger V, Rosamond W, Sacco R, Sorlie P, Stafford R, Thom T, Wasserthiel-Smoller S, Wong ND, Wylie-Rosett J. Heart Disease and Stroke Statistics--2010 Update. A Report From the American Heart Association. Circulation. 2009
3. Ezekowitz JA, Kaul P, Bakal JA, Armstrong PW, Welsh RC, McAlister FA. Declining inhospital mortality and increasing heart failure incidence in elderly patients with first myocardial infarction. J Am Coll Cardiol. 2009; 53:13–20. [PubMed: 19118718]
4. Braunwald E. Epilogue: what do clinicians expect from imagers? J Am Coll Cardiol. 2006; 47:C101–3. [PubMed: 16631504]
5. Adamu U, Knollmann D, Alrawashdeh W, Almutairi B, Deserno V, Kleinhans E, Schafer W, Hoffmann R. Results of interventional treatment of stress positive coronary artery disease. Am J Cardiol. 2010; 105:1535–1539. [PubMed: 20494657]
6. Boden WE, O'Rourke RA, Teo KK, Hartigan PM, Maron DJ, Kostuk WJ, Knudtson M, Dada M, Casperson P, Harris CL, Chaitman BR, Shaw L, Gosselin G, Nawaz S, Title LM, Gau G, Blaustein AS, Booth DC, Bates ER, Spertus JA, Berman DS, Mancini GB, Weintraub WS. Optimal medical therapy with or without PCI for stable coronary disease. N Engl J Med. 2007; 356:1503–1516. [PubMed: 17387127]
7. Henderson RA, Pocock SJ, Clayton TC, Knight R, Fox KA, Julian DG, Chamberlain DA. Seven-year outcome in the RITA-2 trial: coronary angioplasty versus medical therapy. J Am Coll Cardiol. 2003; 42:1161–1170. [PubMed: 14522473]
8. Virmani R, Burke AP, Farb A, Kolodgie FD. Pathology of the vulnerable plaque. J Am Coll Cardiol. 2006; 47:C13–8. [PubMed: 16631505]

9. Fuster V, Fayad ZA, Moreno PR, Poon M, Corti R, Badimon JJ. Atherothrombosis and high-risk plaque: Part II: approaches by noninvasive computed tomographic/magnetic resonance imaging. J Am Coll Cardiol. 2005; 46:1209–1218. [PubMed: 16198833]
10. Matter CM, Stuber M, Nahrendorf M. Imaging of the unstable plaque: how far have we got? Eur Heart J. 2009; 30:2566–2574. [PubMed: 19833636]
11. Ross R. Atherosclerosis--an inflammatory disease. N Engl J Med. 1999; 340:115–126. [PubMed: 9887164]
12. Libby P. Inflammation in atherosclerosis. Nature. 2002; 420:868–874. [PubMed: 12490960]
13. Rosenfeld ME, Averill MM, Bennett BJ, Schwartz SM. Progression and disruption of advanced atherosclerotic plaques in murine models. Curr Drug Targets. 2008; 9:210–216. [PubMed: 18336239]
14. Schwartz SM, Galis ZS, Rosenfeld ME, Falk E. Plaque rupture in humans and mice. Arterioscler Thromb Vasc Biol. 2007; 27:705–713. [PubMed: 17332493]
15. Alsheikh-Ali AA, Kitsios GD, Balk EM, Lau J, Ip S. The vulnerable atherosclerotic plaque: scope of the literature. Ann Intern Med. 2010; 153:387–395. [PubMed: 20713770]
16. Sanz J, Fayad ZA. Imaging of atherosclerotic cardiovascular disease. Nature. 2008; 451:953–957. [PubMed: 18288186]
17. Nahrendorf M, Keliher E, Panizzi P, Zhang H, Hembrador S, Figueiredo JL, Aikawa E, Kelly K, Libby P, Weissleder R. 18F-4V for PET-CT imaging of VCAM-1 expression in atherosclerosis. JACC Cardiovasc Imaging. 2009; 2:1213–1222. [PubMed: 19833312]
18. Kaufmann BA, Sanders JM, Davis C, Xie A, Aldred P, Sarembock IJ, Lindner JR. Molecular imaging of inflammation in atherosclerosis with targeted ultrasound detection of vascular cell adhesion molecule-1. Circulation. 2007; 116:276–284. [PubMed: 17592078]
19. Nahrendorf M, Jaffer FA, Kelly KA, Sosnovik DE, Aikawa E, Libby P, Weissleder R. Noninvasive vascular cell adhesion molecule-1 imaging identifies inflammatory activation of cells in atherosclerosis. Circulation. 2006; 114:1504–1511. [PubMed: 17000904]
20. Cormode DP, Skajaa T, Fayad ZA, Mulder WJ. Nanotechnology in medical imaging: probe design and applications. Arterioscler Thromb Vasc Biol. 2009; 29:992–1000. [PubMed: 19057023]
21. Lipinski MJ, Frias JC, Amirbekian V, Briley-Saebo KC, Mani V, Samber D, Abbate A, Aguinaldo JG, Massey D, Fuster V, Vetrovec GW, Fayad ZA. Macrophage-specific lipid-based nanoparticles improve cardiac magnetic resonance detection and characterization of human atherosclerosis. JACC Cardiovasc Imaging. 2009; 2:637–647. [PubMed: 19442953]
22. Briley-Saebo KC, Mani V, Hyafil F, Cornily JC, Fayad ZA. Fractionated Feridex and positive contrast: in vivo MR imaging of atherosclerosis. Magn Reson Med. 2008; 59:721–730. [PubMed: 18383304]
23. Kooi ME, Cappendijk VC, Cleutjens KB, Kessels AG, Kitslaar PJ, Borgers M, Frederik PM, Daemen MJ, van Engelshoven JM. Accumulation of ultrasmall superparamagnetic particles of iron oxide in human atherosclerotic plaques can be detected by in vivo magnetic resonance imaging. Circulation. 2003; 107:2453–2458. [PubMed: 12719280]
24. Tang TY, Howarth SP, Miller SR, Graves MJ, Patterson AJ, U-King-Im JM, Li ZY, Walsh SR, Brown AP, Kirkpatrick PJ, Warburton EA, Hayes PD, Varty K, Boyle JR, Gaunt ME, Zalewski A, Gillard JH. The ATHEROMA (Atorvastatin Therapy: Effects on Reduction of Macrophage Activity) Study. Evaluation using ultrasmall superparamagnetic iron oxide-enhanced magnetic resonance imaging in carotid disease. J Am Coll Cardiol. 2009; 53:2039–2050. [PubMed: 19477353]
25. Devaraj NK, Keliher EJ, Thurber GM, Nahrendorf M, Weissleder R. 18F labeled nanoparticles for in vivo PET-CT imaging. Bioconjug Chem. 2009; 20:397–401. [PubMed: 19138113]
26. Nahrendorf M, Zhang H, Hembrador S, Panizzi P, Sosnovik DE, Aikawa E, Libby P, Swirski FK, Weissleder R. Nanoparticle PET-CT imaging of macrophages in inflammatory atherosclerosis. Circulation. 2008; 117:379–387. [PubMed: 18158358]
27. Schafers M, Riemann B, Kopka K, Breyholz HJ, Wagner S, Schafers KP, Law MP, Schober O, Levkau B. Scintigraphic imaging of matrix metalloproteinase activity in the arterial wall in vivo. Circulation. 2004; 109:2554–2559. [PubMed: 15123523]

28. Zhang J, Nie L, Razavian M, Ahmed M, Dobrucki LW, Asadi A, Edwards DS, Azure M, Sinusas AJ, Sadeghi MM. Molecular imaging of activated matrix metalloproteinases in vascular remodeling. Circulation. 2008; 118:1953–1960. [PubMed: 18936327]
29. Chen J, Tung CH, Mahmood U, Ntziachristos V, Gyurko R, Fishman MC, Huang PL, Weissleder R. In vivo imaging of proteolytic activity in atherosclerosis. Circulation. 2002; 105:2766–2771. [PubMed: 12057992]
30. Nahrendorf M, Waterman P, Thurber G, Groves K, Rajopadhye M, Panizzi P, Marinelli B, Aikawa E, Pittet MJ, Swirski FK, Weissleder R. Hybrid in vivo FMT-CT imaging of protease activity in atherosclerosis with customized nanosensors. Arterioscler Thromb Vasc Biol. 2009; 29:1444–1451. [PubMed: 19608968]
31. Weissleder R, Ntziachristos V. Shedding light onto live molecular targets. Nat Med. 2003; 9:123–128. [PubMed: 12514725]
32. Jaffer FA, Vinegoni C, John MC, Aikawa E, Gold HK, Finn AV, Ntziachristos V, Libby P, Weissleder R. Real-time catheter molecular sensing of inflammation in proteolytically active atherosclerosis. Circulation. 2008; 118:1802–1809. [PubMed: 18852366]
33. Razansky RN, Rosenthal A, Mallas G, Razansky D, Jaffer FA, Ntziachristos V. Near-infrared fluorescence catheter system for two-dimensional intravascular imaging in vivo. Opt Express. 2010; 18:11372–11381. [PubMed: 20588998]
34. Zhang J, Krassilnikova S, Gharaei AA, Fassaei HR, Esmailzadeh L, Asadi A, Edwards DS, Harris TD, Azure M, Tellides G, Sinusas AJ, Zaret BL, Bender JR, Sadeghi MM. Alphavbeta3-targeted detection of arteriopathy in transplanted human coronary arteries: an autoradiographic study. FASEB J. 2005; 19:1857–1859. [PubMed: 16150802]
35. Sadeghi MM, Krassilnikova S, Zhang J, Gharaei AA, Fassaei HR, Esmailzadeh L, Kooshkabadi A, Edwards S, Yalamanchili P, Harris TD, Sinusas AJ, Zaret BL, Bender JR. Detection of injury-induced vascular remodeling by targeting activated alphavbeta3 integrin in vivo. Circulation. 2004; 110:84–90. [PubMed: 15210600]
36. Winter PM, Morawski AM, Caruthers SD, Fuhrhop RW, Zhang H, Williams TA, Allen JS, Lacy EK, Robertson JD, Lanza GM, Wickline SA. Molecular imaging of angiogenesis in early-stage atherosclerosis with alpha(v)beta3-integrin-targeted nanoparticles. Circulation. 2003; 108:2270–2274. [PubMed: 14557370]
37. Ronald JA, Chen JW, Chen Y, Hamilton AM, Rodriguez E, Reynolds F, Hegele RA, Rogers KA, Querol M, Bogdanov A, Weissleder R, Rutt BK. Enzyme-sensitive magnetic resonance imaging targeting myeloperoxidase identifies active inflammation in experimental rabbit atherosclerotic plaques. Circulation. 2009; 120:592–599. [PubMed: 19652086]
38. Spuentrup E, Katoh M, Wiethoff AJ, Buecker A, Botnar RM, Parsons EC, Guenther RW. Molecular coronary MR imaging of human thrombi using EP-2104R, a fibrin-targeted contrast agent: experimental study in a swine model. Rofo. 2007; 179:1166–1173. [PubMed: 17948194]
39. von zur Muhlen C, von Elverfeldt D, Moeller JA, Choudhury RP, Paul D, Hagemeyer CE, Olschewski M, Becker A, Neudorfer I, Bassler N, Schwarz M, Bode C, Peter K. Magnetic resonance imaging contrast agent targeted toward activated platelets allows in vivo detection of thrombosis and monitoring of thrombolysis. Circulation. 2008; 118:258–267. [PubMed: 18574047]
40. Klink A, Lancelot E, Ballet S, Vucic E, Fabre JE, Gonzalez W, Medina C, Corot C, Mulder WJ, Mallat Z, Fayad ZA. Magnetic resonance molecular imaging of thrombosis in an arachidonic acid mouse model using an activated platelet targeted probe. Arterioscler Thromb Vasc Biol. 2010; 30:403–410. [PubMed: 20139362]
41. Briley-Saebo KC, Shaw PX, Mulder WJ, Choi SH, Vucic E, Aguinaldo JG, Witztum JL, Fuster V, Tsimikas S, Fayad ZA. Targeted molecular probes for imaging atherosclerotic lesions with magnetic resonance using antibodies that recognize oxidation-specific epitopes. Circulation. 2008; 117:3206–3215. [PubMed: 18541740]
42. Rudd JH, Narula J, Strauss HW, Virmani R, Machac J, Klimas M, Tahara N, Fuster V, Warburton EA, Fayad ZA, Tawakol AA. Imaging atherosclerotic plaque inflammation by fluorodeoxyglucose with positron emission tomography: ready for prime time? J Am Coll Cardiol. 2010; 55:2527–2535. [PubMed: 20513592]

43. Rogers IS, Nasir K, Figueroa AL, Cury RC, Hoffmann U, Vermylen DA, Brady TJ, Tawakol A. Feasibility of FDG imaging of the coronary arteries: comparison between acute coronary syndrome and stable angina. JACC Cardiovasc Imaging. 2010; 3:388–397. [PubMed: 20394901]
44. Wykrzykowska J, Lehman S, Williams G, Parker JA, Palmer MR, Varkey S, Kolodny G, Laham R. Imaging of inflamed and vulnerable plaque in coronary arteries with 18F-FDG PET/CT in patients with suppression of myocardial uptake using a low-carbohydrate, high-fat preparation. J Nucl Med. 2009; 50:563–568. [PubMed: 19289431]
45. Kelloff GJ, Hoffman JM, Johnson B, Scher HI, Siegel BA, Cheng EY, Cheson BD, O'shaughnessy J, Guyton KZ, Mankoff DA, Shankar L, Larson SM, Sigman CC, Schilsky RL, Sullivan DC. Progress and promise of FDG-PET imaging for cancer patient management and oncologic drug development. Clin Cancer Res. 2005; 11:2785–2808. [PubMed: 15837727]
46. Tawakol A, Migrino RQ, Hoffmann U, Abbara S, Houser S, Gewirtz H, Muller JE, Brady TJ, Fischman AJ. Noninvasive in vivo measurement of vascular inflammation with F-18 fluorodeoxyglucose positron emission tomography. J Nucl Cardiol. 2005; 12:294–301. [PubMed: 15944534]
47. Tawakol A, Migrino RQ, Bashian GG, Bedri S, Vermylen D, Cury RC, Yates D, LaMuraglia GM, Furie K, Houser S, Gewirtz H, Muller JE, Brady TJ, Fischman AJ. In vivo 18F-fluorodeoxyglucose positron emission tomography imaging provides a noninvasive measure of carotid plaque inflammation in patients. J Am Coll Cardiol. 2006; 48:1818–1824. [PubMed: 17084256]
48. Hyafil F, Cornily JC, Feig JE, Gordon R, Vucic E, Amirbekian V, Fisher EA, Fuster V, Feldman LJ, Fayad ZA. Noninvasive detection of macrophages using a nanoparticulate contrast agent for computed tomography. Nat Med. 2007; 13:636–641. [PubMed: 17417649]
49. Cormode DP, Roessl E, Thran A, Skajaa T, Gordon RE, Schlomka JP, Fuster V, Fisher EA, Mulder WJ, Proksa R, Fayad ZA. Atherosclerotic Plaque Composition: Analysis with Multicolor CT and Targeted Gold Nanoparticles. Radiology. 2010; 256:774–782. [PubMed: 20668118]
50. Gerber TC, Carr JJ, Arai AE, Dixon RL, Ferrari VA, Gomes AS, Heller GV, McCollough CH, McNitt-Gray MF, Mettler FA, Mieres JH, Morin RL, Yester MV. Ionizing radiation in cardiac imaging: a science advisory from the American Heart Association Committee on Cardiac Imaging of the Council on Clinical Cardiology and Committee on Cardiovascular Imaging and Intervention of the Council on Cardiovascular Radiology and Intervention. Circulation. 2009; 119:1056–1065. [PubMed: 19188512]
51. Kajander S, Joutsiniemi E, Saraste M, Pietila M, Ukkonen H, Saraste A, Sipila HT, Teras M, Maki M, Airaksinen J, Hartiala J, Knuuti J. Cardiac positron emission tomography/computed tomography imaging accurately detects anatomically and functionally significant coronary artery disease. Circulation. 2010; 122:603–613. [PubMed: 20660808]
52. Waxman S, Ishibashi F, Muller JE. Detection and treatment of vulnerable plaques and vulnerable patients: novel approaches to prevention of coronary events. Circulation. 2006; 114:2390–2411. [PubMed: 17130356]
53. Burke AP, Farb A, Malcom GT, Liang YH, Smialek J, Virmani R. Coronary risk factors and plaque morphology in men with coronary disease who died suddenly. N Engl J Med. 1997; 336:1276–1282. [PubMed: 9113930]
54. Kim SH, Hong MK, Park DW, Lee SW, Kim YH, Lee CW, Kim JJ, Park SW, Park SJ. Impact of plaque characteristics analyzed by intravascular ultrasound on long-term clinical outcomes. Am J Cardiol. 2009; 103:1221–1226. [PubMed: 19406263]
55. Marwick TH, Schwaiger M. The future of cardiovascular imaging in the diagnosis and management of heart failure, part 2: clinical applications. Circ Cardiovasc Imaging. 2008; 1:162–170. [PubMed: 19808534]
56. Hofstra L, Liem IH, Dumont EA, Boersma HH, van Heerde WL, Doevendans PA, De Muinck E, Wellens HJ, Kemerink GJ, Reutelingsperger CP, Heidendal GA. Visualisation of cell death in vivo in patients with acute myocardial infarction. Lancet. 2000; 356:209–212. [PubMed: 10963199]
57. Sosnovik DE, Schellenberger EA, Nahrendorf M, Novikov MS, Matsui T, Dai G, Reynolds F, Grazette L, Rosenzweig A, Weissleder R, Josephson L. Magnetic resonance imaging of cardiomyocyte apoptosis with a novel magneto-optical nanoparticle. Magn Reson Med. 2005; 54:718–724. [PubMed: 16086367]

58. Hiller KH, Waller C, Nahrendorf M, Bauer WR, Jakob PM. Assessment of cardiovascular apoptosis in the isolated rat heart by magnetic resonance molecular imaging. Mol Imaging. 2006; 5:115–121. [PubMed: 16954025]
59. Sosnovik DE, Nahrendorf M, Panizzi P, Matsui T, Aikawa E, Dai G, Li L, Reynolds F, Dorn GWn, Weissleder R, Josephson L, Rosenzweig A. Molecular MRI detects low levels of cardiomyocyte apoptosis in a transgenic model of chronic heart failure. Circ Cardiovasc Imaging. 2009; 2:468–475. [PubMed: 19920045]
60. Sosnovik DE, Garanger E, Aikawa E, Nahrendorf M, Figuiredo JL, Dai G, Reynolds F, Rosenzweig A, Weissleder R, Josephson L. Molecular MRI of cardiomyocyte apoptosis with simultaneous delayed-enhancement MRI distinguishes apoptotic and necrotic myocytes in vivo: potential for midmyocardial salvage in acute ischemia. Circ Cardiovasc Imaging. 2009; 2:460–467. [PubMed: 19920044]
61. Garanger E, Hilderbrand SA, Blois JT, Sosnovik DE, Weissleder R, Josephson L. A DNA-binding Gd chelate for the detection of cell death by MRI. Chem Commun (Camb). 2009:4444–4446. [PubMed: 19597620]
62. Kietselaer BL, Reutelingsperger CP, Boersma HH, Heidendal GA, Liem IH, Crijns HJ, Narula J, Hofstra L. Noninvasive detection of programmed cell loss with 99mTc-labeled annexin A5 in heart failure. J Nucl Med. 2007; 48:562–567. [PubMed: 17401092]
63. Frangogiannis NG, Smith CW, Entman ML. The inflammatory response in myocardial infarction. Cardiovasc Res. 2002; 53:31–47. [PubMed: 11744011]
64. Swirski FK, Nahrendorf M, Etzrodt M, Wildgruber M, Cortez-Retamozo V, Panizzi P, Figueiredo JL, Kohler RH, Chudnovskiy A, Waterman P, Aikawa E, Mempel TR, Libby P, Weissleder R, Pittet MJ. Identification of splenic reservoir monocytes and their deployment to inflammatory sites. Science. 2009; 325:612–616. [PubMed: 19644120]
65. Nahrendorf M, Pittet MJ, Swirski FK. Monocytes: protagonists of infarct inflammation and repair after myocardial infarction. Circulation. 2010; 121:2437–2445. [PubMed: 20530020]
66. Nahrendorf M, Swirski FK, Aikawa E, Stangenberg L, Wurdinger T, Figueiredo JL, Libby P, Weissleder R, Pittet MJ. The healing myocardium sequentially mobilizes two monocyte subsets with divergent and complementary functions. J Exp Med. 2007; 204:3037–3047. [PubMed: 18025128]
67. Tsujioka H, Imanishi T, Ikejima H, Kuroi A, Takarada S, Tanimoto T, Kitabata H, Okochi K, Arita Y, Ishibashi K, Komukai K, Kataiwa H, Nakamura N, Hirata K, Tanaka A, Akasaka T. Impact of heterogeneity of human peripheral blood monocyte subsets on myocardial salvage in patients with primary acute myocardial infarction. J Am Coll Cardiol. 2009; 54:130–138. [PubMed: 19573729]
68. Panizzi P, Swirski FK, Figueiredo JL, Waterman P, Sosnovik DE, Aikawa E, Libby P, Pittet M, Weissleder R, Nahrendorf M. Impaired infarct healing in atherosclerotic mice with Ly-6C(hi) monocytosis. J Am Coll Cardiol. 2010; 55:1629–1638. [PubMed: 20378083]
69. Sosnovik DE, Nahrendorf M, Deliolanis N, Novikov M, Aikawa E, Josephson L, Rosenzweig A, Weissleder R, Ntziachristos V. Fluorescence tomography and magnetic resonance imaging of myocardial macrophage infiltration in infarcted myocardium in vivo. Circulation. 2007; 115:1384–1391. [PubMed: 17339546]
70. Nahrendorf M, Sosnovik DE, Waterman P, Swirski FK, Pande AN, Aikawa E, Figueiredo JL, Pittet MJ, Weissleder R. Dual channel optical tomographic imaging of leukocyte recruitment and protease activity in the healing myocardial infarct. Circ Res. 2007; 100:1218–1225. [PubMed: 17379832]
71. Flogel U, Ding Z, Hardung H, Jander S, Reichmann G, Jacoby C, Schubert R, Schrader J. In vivo monitoring of inflammation after cardiac and cerebral ischemia by fluorine magnetic resonance imaging. Circulation. 2008; 118:140–148. [PubMed: 18574049]
72. Berr SS, Xu Y, Roy RJ, Kundu B, Williams MB, French BA. Images in cardiovascular medicine. Serial multimodality assessment of myocardial infarction in mice using magnetic resonance imaging and micro-positron emission tomography provides complementary information on the progression of scar formation. Circulation. 2007; 115:e428–9. [PubMed: 17470701]
73. Peterson LR, Gropler RJ. Radionuclide imaging of myocardial metabolism. Circ Cardiovasc Imaging. 2010; 3:211–222. [PubMed: 20233863]

74. Nahrendorf M, Keliher E, Marinelli B, Waterman P, Feruglio PF, Fexon L, Pivovarov M, Swirski FK, Pittet MJ, Vinegoni C, Weissleder R. Hybrid PET-optical imaging using targeted probes. Proc Natl Acad Sci U S A. 2010; 107:7910–7915. [PubMed: 20385821]
75. Christiansen JP, Leong-Poi H, Klibanov AL, Kaul S, Lindner JR. Noninvasive imaging of myocardial reperfusion injury using leukocyte-targeted contrast echocardiography. Circulation. 2002; 105:1764–1767. [PubMed: 11956115]
76. Ertl G, Frantz S. Healing after myocardial infarction. Cardiovasc Res. 2005; 66:22–32. [PubMed: 15769445]
77. Lindsey ML, Zamilpa R. Temporal and Spatial Expression of Matrix Metalloproteinases and Tissue Inhibitors of Metalloproteinases Following Myocardial Infarction. Cardiovasc Ther. 2010
78. Spinale FG. Myocardial matrix remodeling and the matrix metalloproteinases: influence on cardiac form and function. Physiol Rev. 2007; 87:1285–1342. [PubMed: 17928585]
79. Su H, Spinale FG, Dobrucki LW, Song J, Hua J, Sweterlitsch S, Dione DP, Cavaliere P, Chow C, Bourke BN, Hu XY, Azure M, Yalamanchili P, Liu R, Cheesman EH, Robinson S, Edwards DS, Sinusas AJ. Noninvasive targeted imaging of matrix metalloproteinase activation in a murine model of postinfarction remodeling. Circulation. 2005; 112:3157–3167. [PubMed: 16275862]
80. Chen J, Tung CH, Allport JR, Chen S, Weissleder R, Huang PL. Near-infrared fluorescent imaging of matrix metalloproteinase activity after myocardial infarction. Circulation. 2005; 111:1800–1805. [PubMed: 15809374]
81. Nahrendorf M, Sosnovik D, Chen JW, Panizzi P, Figueiredo JL, Aikawa E, Libby P, Swirski FK, Weissleder R. Activatable magnetic resonance imaging agent reports myeloperoxidase activity in healing infarcts and noninvasively detects the antiinflammatory effects of atorvastatin on ischemia-reperfusion injury. Circulation. 2008; 117:1153–1160. [PubMed: 18268141]
82. Swirski FK, Wildgruber M, Ueno T, Figueiredo JL, Panizzi P, Iwamoto Y, Zhang E, Stone JR, Rodriguez E, Chen JW, Pittet MJ, Weissleder R, Nahrendorf M. Myeloperoxidase-rich Ly-6C+ myeloid cells infiltrate allografts and contribute to an imaging signature of organ rejection in mice. J Clin Invest. 2010; 120:2627–2634. [PubMed: 20577051]
83. Chen JW, Querol Sans M, Bogdanov AJ, Weissleder R. Imaging of myeloperoxidase in mice by using novel amplifiable paramagnetic substrates. Radiology. 2006; 240:473–481. [PubMed: 16864673]
84. Panizzi P, Nahrendorf M, Wildgruber M, Waterman P, Figueiredo JL, Aikawa E, McCarthy J, Weissleder R, Hilderbrand SA. Oxazine conjugated nanoparticle detects in vivo hypochlorous acid and peroxynitrite generation. J Am Chem Soc. 2009; 131:15739–15744. [PubMed: 19817443]
85. van den Borne SW, Isobe S, Verjans JW, Petrov A, Lovhaug D, Li P, Zandbergen HR, Ni Y, Frederik P, Zhou J, Arbo B, Rogstad A, Cuthbertson A, Chettibi S, Reutelingsperger C, Blankesteijn WM, Smits JF, Daemen MJ, Zannad F, Vannan MA, Narula N, Pitt B, Hofstra L, Narula J. Molecular imaging of interstitial alterations in remodeling myocardium after myocardial infarction. J Am Coll Cardiol. 2008; 52:2017–2028. [PubMed: 19055994]
86. Verjans J, Wolters S, Laufer W, Schellings M, Lax M, Lovhaug D, Boersma H, Kemerink G, Schalla S, Gordon P, Teule J, Narula J, Hofstra L. Early molecular imaging of interstitial changes in patients after myocardial infarction: Comparison with delayed contrast-enhanced magnetic resonance imaging. J Nucl Cardiol. 2010
87. Makowski MR, Ebersberger U, Nekolla S, Schwaiger M. In vivo molecular imaging of angiogenesis, targeting alphavbeta3 integrin expression, in a patient after acute myocardial infarction. Eur Heart J. 2008; 29:2201. [PubMed: 18375397]
88. Meoli DF, Sadeghi MM, Krassilnikova S, Bourke BN, Giordano FJ, Dione DP, Su H, Edwards DS, Liu S, Harris TD, Madri JA, Zaret BL, Sinusas AJ. Noninvasive imaging of myocardial angiogenesis following experimental myocardial infarction. J Clin Invest. 2004; 113:1684–1691. [PubMed: 15199403]
89. Nahrendorf M, Sosnovik DE, French BA, Swirski FK, Bengel F, Sadeghi MM, Lindner JR, Wu JC, Kraitchman DL, Fayad ZA, Sinusas AJ. Multimodality cardiovascular molecular imaging, Part II. Circ Cardiovasc Imaging. 2009; 2:56–70. [PubMed: 19808565]
90. McDonald DM, Choyke PL. Imaging of angiogenesis: from microscope to clinic. Nat Med. 2003; 9:713–725. [PubMed: 12778170]

91. Nahrendorf M, Hu K, Frantz S, Jaffer FA, Tung CH, Hiller KH, Voll S, Nordbeck P, Sosnovik D, Gattenlohner S, Novikov M, Dickneite G, Reed GL, Jakob P, Rosenzweig A, Bauer WR, Weissleder R, Ertl G. Factor XIII deficiency causes cardiac rupture, impairs wound healing, and aggravates cardiac remodeling in mice with myocardial infarction. Circulation. 2006; 113:1196–1202. [PubMed: 16505171]
92. Nahrendorf M, Aikawa E, Figueiredo JL, Stangenberg L, van den Borne SW, Blankesteijn WM, Sosnovik DE, Jaffer FA, Tung CH, Weissleder R. Transglutaminase activity in acute infarcts predicts healing outcome and left ventricular remodelling: implications for FXIII therapy and antithrombin use in myocardial infarction. Eur Heart J. 2008; 29:445–454. [PubMed: 18276618]
93. Gemmati D, Federici F, Campo G, Tognazzo S, Serino ML, De Mattei M, Valgimigli M, Malagutti P, Guardigli G, Ferraresi P, Bernardi F, Ferrari R, Scapoli GL, Catozzi L. Factor XIIIA-V34L and factor XIIIB-H95R gene variants: effects on survival in myocardial infarction patients. Mol Med. 2007; 13:112–120. [PubMed: 17515963]
94. Helm PA, Caravan P, French BA, Jacques V, Shen L, Xu Y, Beyers RJ, Roy RJ, Kramer CM, Epstein FH. Postinfarction myocardial scarring in mice: molecular MR imaging with use of a collagen-targeting contrast agent. Radiology. 2008; 247:788–796. [PubMed: 18403626]
95. Caravan P, Das B, Dumas S, Epstein FH, Helm PA, Jacques V, Koerner S, Kolodziej A, Shen L, Sun WC, Zhang Z. Collagen-targeted MRI contrast agent for molecular imaging of fibrosis. Angew Chem Int Ed Engl. 2007; 46:8171–8173. [PubMed: 17893943]
96. Verjans JW, Lovhaug D, Narula N, Petrov AD, Indrevoll B, Bjurgert E, Krasieva TB, Petersen LB, Kindberg GM, Solbakken M, Cuthbertson A, Vannan MA, Reutelingsperger CP, Tromberg BJ, Hofstra L, Narula J. Noninvasive imaging of angiotensin receptors after myocardial infarction. JACC Cardiovasc Imaging. 2008; 1:354–362. [PubMed: 19356449]
97. Ungerer M, Hartmann F, Karoglan M, Chlistalla A, Ziegler S, Richardt G, Overbeck M, Meisner H, Schomig A, Schwaiger M. Regional in vivo and in vitro characterization of autonomic innervation in cardiomyopathic human heart. Circulation. 1998; 97:174–180. [PubMed: 9445170]
98. Link JM, Stratton JR, Levy W, Poole JE, Shoner SC, Stuetzle W, Caldwell JH. PET measures of pre- and post-synaptic cardiac beta adrenergic function. Nucl Med Biol. 2003; 30:795–803. [PubMed: 14698782]
99. Leuschner F, Panizzi P, Chico-Calero I, Lee WW, Ueno T, Cortez-Retamozo V, Waterman P, Gorbatov R, Marinelli B, Iwamoto Y, Chudnovskiy A, Figueiredo JL, Sosnovik DE, Pittet MJ, Swirski FK, Weissleder R, Nahrendorf M. Angiotensin-Converting Enzyme Inhibition Prevents the Release of Monocytes From Their Splenic Reservoir in Mice With Myocardial Infarction. Circ Res. 2010
100. Scherrer-Crosbie M, Kurtz B. Ventricular remodeling and function: insights using murine echocardiography. J Mol Cell Cardiol. 2010; 48:512–517. [PubMed: 19615377]
101. Weissleder R, Pittet MJ. Imaging in the era of molecular oncology. Nature. 2008; 452:580–589. [PubMed: 18385732]
102. Schulz RB, Ale A, Sarantopoulos A, Freyer M, Soehngen E, Zientkowska M, Ntziachristos V. Hybrid system for simultaneous fluorescence and x-ray computed tomography. IEEE Trans Med Imaging. 2010; 29:465–473. [PubMed: 19906585]
103. Ntziachristos V. Going deeper than microscopy: the optical imaging frontier in biology. Nat Methods. 2010; 7:603–614. [PubMed: 20676081]
104. Michalet X, Pinaud FF, Bentolila LA, Tsay JM, Doose S, Li JJ, Sundaresan G, Wu AM, Gambhir SS, Weiss S. Quantum dots for live cells, in vivo imaging, and diagnostics. Science. 2005; 307:538–544. [PubMed: 15681376]
105. Shu X, Royant A, Lin MZ, Aguilera TA, Lev-Ram V, Steinbach PA, Tsien RY. Mammalian expression of infrared fluorescent proteins engineered from a bacterial phytochrome. Science. 2009; 324:804–807. [PubMed: 19423828]
106. Catana C, Procissi D, Wu Y, Judenhofer MS, Qi J, Pichler BJ, Jacobs RE, Cherry SR. Simultaneous in vivo positron emission tomography and magnetic resonance imaging. Proc Natl Acad Sci U S A. 2008; 105:3705–3710. [PubMed: 18319342]
107. Judenhofer MS, Wehrl HF, Newport DF, Catana C, Siegel SB, Becker M, Thielscher A, Kneilling M, Lichy MP, Eichner M, Klingel K, Reischl G, Widmaier S, Rocken M, Nutt RE, Machulla HJ,

Uludag K, Cherry SR, Claussen CD, Pichler BJ. Simultaneous PET-MRI: a new approach for functional and morphological imaging. Nat Med. 2008; 14:459–465. [PubMed: 18376410]

108. Kim HW, Farzaneh-Far A, Kim RJ. Cardiovascular magnetic resonance in patients with myocardial infarction: current and emerging applications. J Am Coll Cardiol. 2009; 55:1–16. [PubMed: 20117357]
109. Rehwald WG, Wagner A, Sievers B, Kim RJ, Judd RM. Cardiovascular MRI: its current and future use in clinical practice. Expert Rev Cardiovasc Ther. 2007; 5:307–321. [PubMed: 17338674]
110. Bandettini WP, Arai AE. Advances in clinical applications of cardiovascular magnetic resonance imaging. Heart. 2008; 94:1485–1495. [PubMed: 18208827]
111. Laitinen I, Saraste A, Weidl E, Poethko T, Weber AW, Nekolla SG, Leppanen P, Yla-Herttuala S, Holzlwimmer G, Walch A, Esposito I, Wester HJ, Knuuti J, Schwaiger M. Evaluation of alphavbeta3 integrin-targeted positron emission tomography tracer 18F-galacto-RGD for imaging of vascular inflammation in atherosclerotic mice. Circ Cardiovasc Imaging. 2009; 2:331–338. [PubMed: 19808614]
112. Stuber M, Weiss RG. Coronary magnetic resonance angiography. J Magn Reson Imaging. 2007; 26:219–234. [PubMed: 17610288]
113. Yu J, Schar M, Vonken EJ, Kelle S, Stuber M. Improved SNR efficiency in gradient echo coronary MRA with high temporal resolution using parallel imaging. Magn Reson Med. 2009; 62:1211–1220. [PubMed: 19780151]
114. Vinegoni C, Razansky D, Figueiredo JL, Fexon L, Pivovarov M, Nahrendorf M, Ntziachristos V, Weissleder R. Born normalization for fluorescence optical projection tomography for whole heart imaging. J Vis Exp. 2009

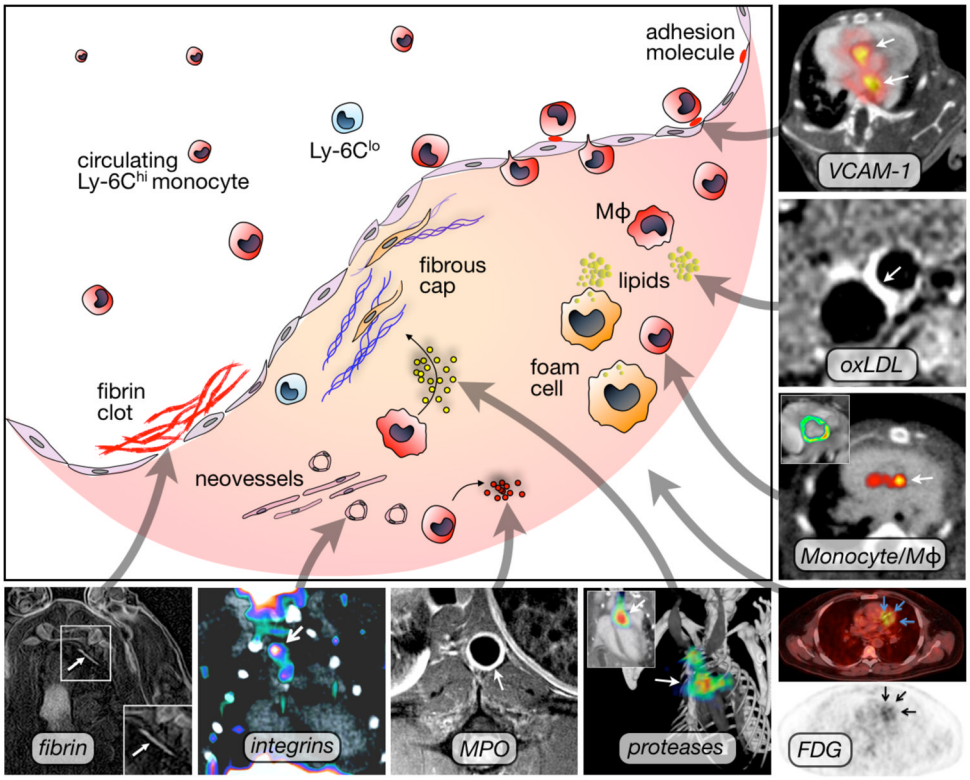

Figure 1. Selected molecular imaging targets in atherosclerosis

VCAM-1: PET-CT imaging of adhesion molecule expression in the root of apoE$^{-/-}$ mice with the tetrameric peptide ^{18}F-4V. Adapted with permission [17].

oxLDL: Gd-loaded microvesicles targeted to oxLDL result in increased T1 MRI contrast. Adapted with permission [41].

Mono/Mac: Quantitation of myeloid cells in atherosclerotic plaque using iron oxide nanoparticles that increase T2* contrast on MRI (inset) and can be used for PET-CT imaging due to labeling with ^{64}Cu. Adapted with permission [26].

FDG: PET-CT imaging of metabolic activity in a patient with coronary heart disease using the glucose analogon ^{18}F-FDG. Adapted with permission [44].

Proteases: FMT-CT imaging of cathepsin protease activity in the root of apoE$^{-/-}$ mice. Adapted with permission [30].

MPO: MR imaging of myeloperoxidase activity in a rabbit model of atherosclerosis. Image courtesy of Dr. John Chen.

Integrins: PET-CT imaging using ^{18}F-Galacto-RGD in LDLr$^{-/-}$ mice. Adapted with permission [111].

Fibrin: MR imaging of fibrin within coronary artery clots in a swine model. Adapted with permission [38].

Mφ: Macrophage.

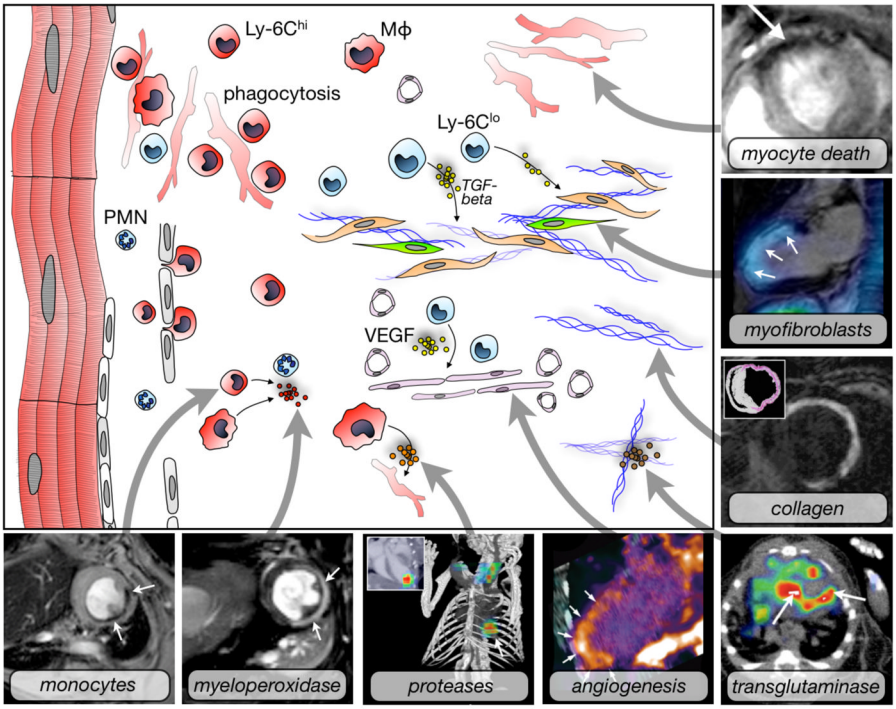

Figure 2. Molecular imaging targets in myocardial infarction

Myocyte death: Use of annexin-V decorated iron oxide nanoparticles in a mouse model of myocardial ischemia results in signal decay (arrow). Adapted with permission [57].

Myofibroblasts: Fused SPECT-MR image shows uptake of an integrin targeted SPECT tracer in the infarct of a patient, delineated by delayed enhancement MRI. Adapted with permission [86].

Collagen: Postinfarction myocardial scarring in mice imaged by MRI with the use of a collagen-targeting agent. The inset shows histological collagen localization in the infarct. Adapted with permission [94].

Transglutaminase: SPECT-CT imaging of factor XIII activity in a mouse with coronary ligation predicts infarct healing and remodeling. Adapted with permission [92].

Angiogenesis: Integrin PET-CT imaging in a patient with MI. Adapted with permission [87].

Proteases: FMT-CT imaging in a murine infarct shows protease activity in the healing myocardium. Adapted with permission [68].

Myeloperoxidase: Use of MPO-Gd in T1-weighted MRI in a mouse with coronary ligation to measure inflammation non-invasively. Adapted with permission [81].

Monocytes: Iron oxide nanoparticles accumulate in monocytes and macrophages in the ischemic myocardium of a mouse. T2* weighted imaging at 7 Tesla. Own, previously unpublished data.

Mφ: Macrophage, PMN: neutrophil.

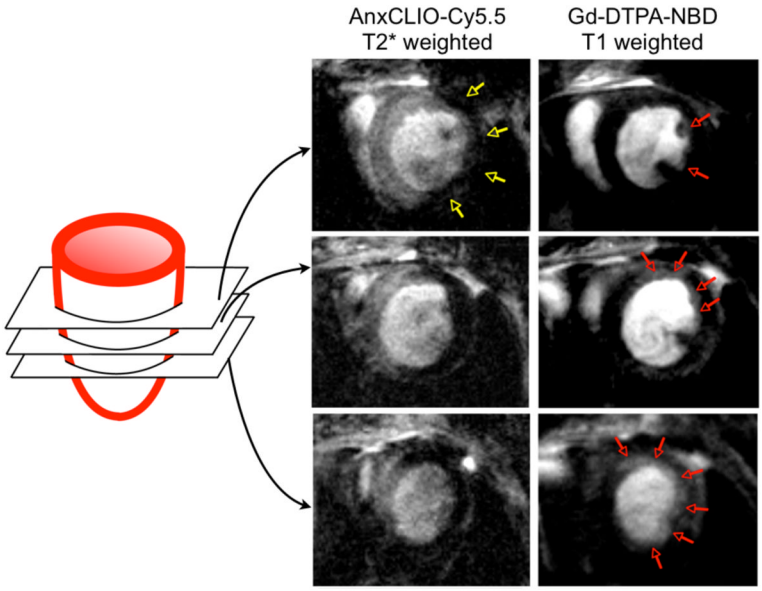

Figure 3. Dual channel MRI of myocyte death

Molecular MRI of apoptotic myocardium (yellow arrows in left column, T2* weighted imaging using an echo time of 4 ms) and simultaneous delayed enhancement MRI of Gd-DTPA (right, T1 weighted imaging with an echo time of 1ms and myocardial signal suppression). At the midventricular level, only a small area in the subendocardium of the lateral wall showed delayed enhancement (red arrows). The extent of delayed enhancement increased progressively in the more apical slices (red arrows) and was fairly extensive at the apex. Adapted with permission [60].

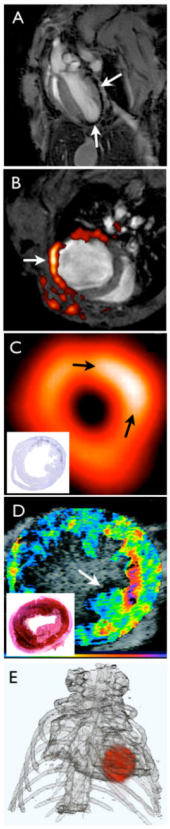

Figure 4. Imaging of monocyte/macrophages in myocardial infarction

(A) T2* weighted MRI of iron oxide nanoparticles in a murine infarct model. Using a long echo time, imaging was done at 7 Tesla and shows the typical proton signal decay caused by interaction of protons with iron oxide (arrows). Own, previously unpublished data.

(B) F19 fluorine MRI merged with proton MR image for anatomic information. Nanoemulsions of perfluorocarbons are taken up by myeloid cells in the infarct. Adapted with permission [71].

(C) ^{18}F-FDG PET image in a mouse 7 days after coronary ligation. In this study, PET signal was higher in the subacute MI (arrows) compared to the remote myocardium, likely due to the enhanced presence of metabolically active monocytes/ macrophages in the infarct. The inset shows the corresponding macrophage stain. Adapted with permission [72].

(D) Molecular ultrasound imaging in a dog model of myocardial ischemia with leukocyte targeted microbubbles. The inset shows the location of the infarct in the corresponding TTC stain. Adapted with permission [75].

(E) FMT-CT reconstruction showing the distribution of a fluorescent sensor in the infarct of a mouse. Own, previously unpublished data, image reconstruction courtesy of Dr. Claudio Vinegoni.

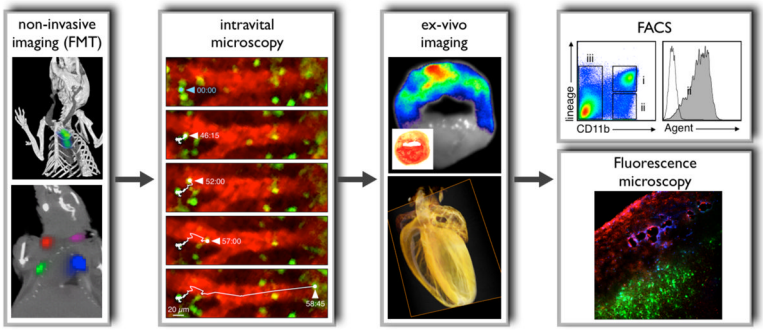

Figure 5. Integrative fluorescence imaging

Non-invasive imaging (FMT): The upper panel shows imaging with FMT-CT in an apoE$^{-/-}$ mouse after injection of an activatable protease reporter. Adapted with permission [30]. The lower panel illustrates spectrally resolved 4-channel FMT-CT imaging in a mouse that was subcutaneously injected with 4 fluorochromes of different excitation/ emission wavelengths. For reconstruction, the 4 channels were color-coded and merged with anatomic CT. Adapted with permission [74].

Intravital microscopy: Dual channel imaging of a fluorescent blood pool marker (red) and monocytes expressing green fluorescent protein in the spleen [64, 99]. The time series shows a monocyte that departs from the organ in a mouse with MI. Adapted with permission [64]. Intravital microscopy imaging in the vessels and the heart is complicated by motion; however, future strategies will suppress motion with tissue stabilizing during acquisition and post processing compensation algorithms.

Ex-vivo imaging: The upper panel shows fluorescence reflectance imaging of a myocardial short axis ring after injection of a protease reporter (inset: TTC stain). Adapted with permission [70]. The lower panel illustrates optical projection tomography (OPT) in a mouse heart [114]. OPT allows to study molecular events in anatomical context and with high resolution. The panel shows a reconstructed image for the absorption coefficient acquired in a mouse heart with 360 projections. Previously unpublished, image courtesy of Dr. Claudio Vinegoni.

FACS: After imaging, target tissue can be minced, digested and filtered to produce cell suspensions which are analyzed by multicolor flow cytometry. The specific example shows leukocyte populations in digested infarct tissue. Gate ii comprises CD11b^{+} lineage^{-} myeloid cells, including monocytes and macrophages. The histogram on he right shows fluorescence in these cells, which reports on uptake of a fluorescent molecular agent. Image courtesy of Dr. Filip Swirski.

Fluorescence microscopy: Alternatively, tissue can be embedded to study signal distribution by fluorescence microscopy. The panel shows distribution of an integrin targeted probe (blue), a protease reporter (red) and nanoparticles targeted to myeloid cells (green) in a tumor model. Adapted with permission [74].

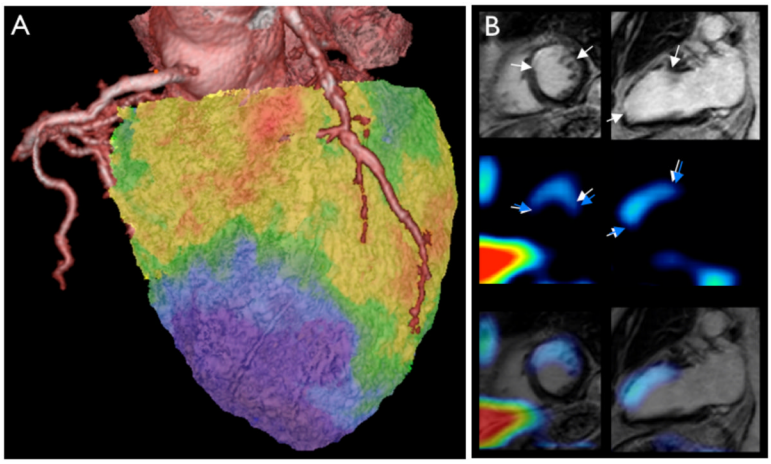

Figure 6. Clinical multimodal imaging

(A) Hybrid X-ray CT angiography fused to ^{18}F-FDG PET for myocardial viability. This patient presented with new onset of heart failure. Severe left ventricular dysfunction with akinesia in the apex, anterior septum, and anterior free wall as well as posterolateral wall was detected in echocardiography. Coronary CT angiography showed chronic occlusion in the proximal LCX, severe stenosis in the proximal LAD and total occlusion of the distal LAD. ^{18}F-FDG PET images demonstrated severe defects in the apex and lateral wall consistent with infarct scar (blue). However, there was preserved ^{18}F-FDG uptake in the septum and most of the anterior wall as well as in the inferior wall consistent with large areas of viable myocardium (green and red colors). Subsequently, the patient underwent successful bypass surgery with venous grafts implanted in the distal LAD, diagonal branch and LCX, which relieved heart failure symptoms. Images and case report are previously unpublished and courtesy of Dr. Juhani Knuuti.

(B) SPECT imaging of integrin expression (3 weeks after ischemia) combined with delayed enhancement MRI (1 year after ischemia) in a patient with myocardial infarction. The first row demonstrates delayed enhancement MR image of scar tissue in the LAD region (white arrows) in short and long axis views. The second row shows slices with technetium-99 uptake (blue arrows). The last row shows SPECT/MR fusion images. Adapted with permission[86].

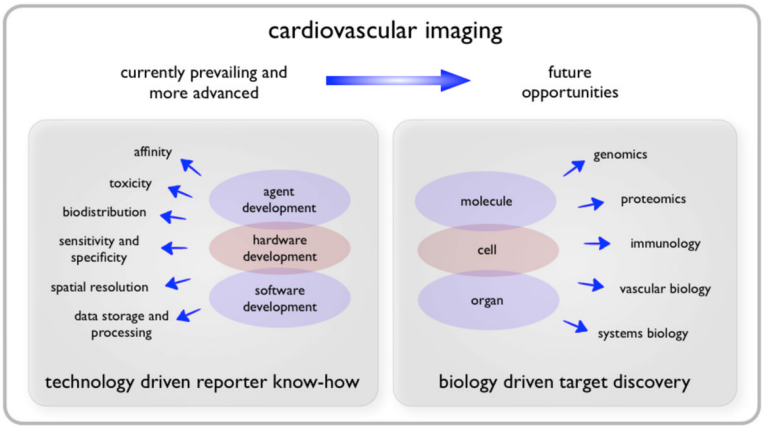

Figure 7. Achievements and opportunities

While the last decade has seen profound progress of cardiovascular imaging technology, which resulted in convincing proof of principle molecular imaging studies in animal models and in patients, our rapidly evolving understanding of biological systems will likely foster discovery of improved imaging targets.

Table 1

Advantages and disadvantages of modalities for molecular imaging of the heart

	Advantages	Disadvantages
Optical	high resolution, may aid intervention, multispectral	invasive (catheter based)
Ultrasound	high spatial resolution, real-time imaging, inexpensive, widely available	inter-observer variability, limitation with adjacent bone or lung structures, not quantitative
CT	high spatial resolution	lower sensitivity, radiation exposure
Nuclear	highest sensitivity, quantitative	low spatial resolution, exposure to radioactivity, expensive
MRI	high sensitivity, high spatial and temporal resolution, functional imaging possible	expensive, metallic implants (currently most pace makers and defibrillators) are contraindication